Chapter 7

Characterisation of the relationship between fractal dimension and branching behaviour in filamentous microbes

7.1 Introduction

The optimisation of industrial fermentation processes involving filamentous microorganisms requires an in-depth knowledge of the relationship between biomass and metabolite production. The specific morphological form adopted by an organism in a certain process, which is dependent on a variety of factors [1], is of critical importance to the clarification of this relationship, as particular phenotypes are associated with maximum productivity. The accurate quantification of phenotypic variation in vegetative mycelia, as a means of process control, is therefore of the utmost importance. In particular, the extent to which an organism forms branches is often of interest in industrial processes, as evidence in the literature suggests that metabolite excretion occurs primarily at hyphal tips [2, 3]. With the advent of image analysis systems, significant progress has been made in furthering the understanding of the relationship between morphology and productivity [4]. However, the accurate quantification of complex morphologies still represents a major challenge in

process optimisation.

At the macroscopic level, the dispersed mycelial morphological form may dominate, or an aggregation of biomass may result in mycelial 'clumps' being predominant. These clumps may develop into dense, approximately spherical pellets, which may be up to several millimetres in diameter. In fermentations of certain microorganisms, such as *Aspergillus oryzae*, there is evidence that pellet-formation is driven by spore agglomeration [5] and, as such, the occurrence of 'free' mycelia may be rare. The characterisation of these complex macro-morphologies represents a far greater challenge to the fungal biotechnologist, as individual hyphae cannot be isolated and enumerated. As such, the accurate determination of the extent of branching of the organism is often impossible. These large aggregates of biomass are conventionally characterised in terms of projected area (A_p), perimeter length (P), circularity ($C = 4\pi A_p P^{-2}$), or various other interpretations thereof [6–8]. As different morphological parameters are often utilised depending on the growth form present, a considerable amount of effort has been expended in designing imaging systems capable of discriminating between these different phenotypes [6, 7]. An alternative approach to morphological quantification employs the use of fractal geometry to characterise the spatial distribution of an organism.

7.1.1 What are fractals?

The term 'fractal' geometry, derived from the Latin *fractus* meaning 'broken' or 'fractured', was first used by Benoît Mandelbrot [9] to describe objects that are 'self-similar' (similar at different scales). More specifically, Mandelbrot described a fractal as '*a rough or fragmented geometric shape that can be split into parts, each of which is (at least approximately) a reduced-size copy of the whole.*' There are many examples of such objects in nature; for example, clouds, mountain ranges, coastlines and snow-flakes. Fractal geometry has also been made use of in art (Fig. 7.1), long before the concept was formalised mathematically.

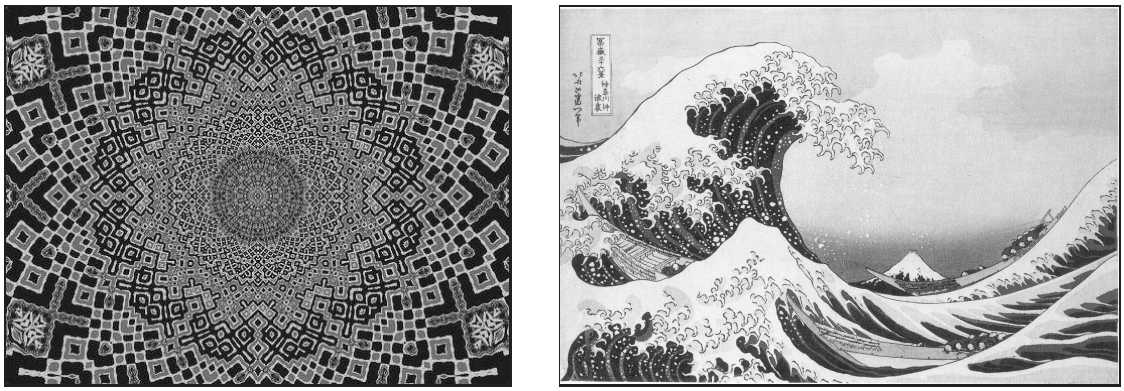

Figure 7.1: Many examples of Islamic art exhibit fractal properties (left), while self-similarity is clearly visible in Hokusai's *The Great Wave off Kanagawa* (right).

Several studies have demonstrated that certain filamentous microorganisms can be considered self-similar structures [10–16], as do several bacterial strains of Gram-negative rods, under certain conditions [17]. Effects of different grazing densities of collembolans on colonies of the fungus *Hypholoma fasciculare* [18] and trophic responses of *Phanerochaete velutina* mycelial systems to nutrient stimuli [19] were also quantified in the same manner. Fractal geometry has also been used as a means of standardising mycelial inocula for submerged fermentations [20].

The concept of fractal or fractional dimension may be considered as follows [21]. Consider a straight line of dimension one and of length X. For any positive integer N, the segment may be exactly decomposed into N non-overlapping segments of length X/N. Each sub-segment may then be considered a scaled version of the original, where $r(N) = 1/N$ is the scaling ratio. This concept may be extended to two dimensions, whereby a rectangle of length X and breadth Y may be sub-divided into N smaller rectangles, each of length $X/\sqrt{N}$ and breadth $Y/\sqrt{N}$, in which case the scaling ratio is $r(N) = 1/\sqrt{N}$. This relationship may be generalised as follows:

$$r(N) = \frac{1}{N^{1/D}} \tag{7.1}$$

The fractal dimension (D) is therefore given by:

$$D = -\frac{\log N}{\log r(N)} \tag{7.2}$$

This principle is illustrated by the construction of the von Koch curves (Fig. 7.2). Beginning with a straight line of length X, the line is divided into three segments, each of length $X/3$. A fourth segment of length $X/3$ is added and the four segments are arrange as shown, producing the triadic von Koch curve. In this case, $r(N) = 1/3$, as each of the individual segments is one third the length of the original, and $N = 4$. Therfore:

$$D = -\frac{\log 4}{\log 1/3} = \frac{\log 4}{\log 3} \approx 1.262$$

Alternatively, if $r(N) = 1/4$ and $N = 8$, the result is the quadratic von Koch curve, for which $D = 1.5$. Iteratively repeating this 'divide and construct' procedure results in curves of increasing visual complexity, which are not easily described using Euclidean measures. However, the basis for their construction is relatively simple, as is their subsequent decomposition into elementary, geometrically identical sub-structures, and a single dimension (D) may be used to describe the curves.

7.1.2 Quantifying the fractal dimension

One of the earlier approaches to fractal dimension quantification, termed the 'Richardson walk' [22], originally described the effect of scale when measuring a coastal perimeter on a map using dividers. As the step size (s) is reduced, the measured perimeter (P) increases, with more of the coastal irregularities included in the measure. A plot of $\log P(s)$ versus $\log n$ will result in a straight line, the slope of which is related to the fractal dimension (D) by:

$$P(s) = as^{1-D} \tag{7.3}$$

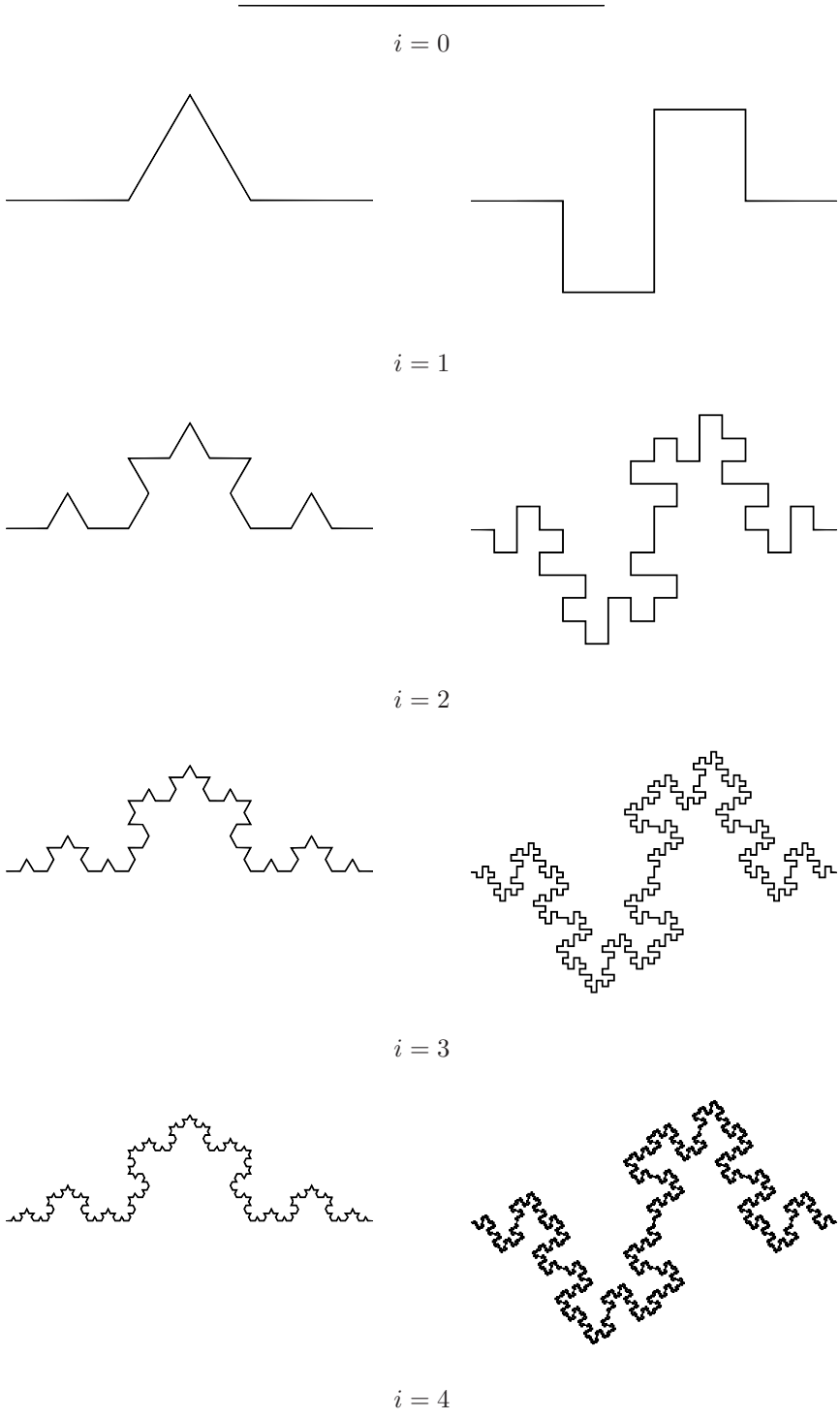

Figure 7.2: The triadic (left) and quadratic (right) von Koch curves, where i denotes the number of iterations.

where a is a constant. The range of scales over which the relationship holds true is obviously limited at the lower end by the resolution of the map and at the upper end by the size of the coastline being measured.

A more accurate implementation of such a method for the analysis of objects in digital images is based on the calculation of a Euclidean distance map (EDM) [23]. The grey-level histogram ($h(x)$) provides the luminance value at each distance (d) from the 'ultimate point', the centre of the EDM. The perimeter, P, at a distance d from the object's centre may be calculated according to:

$$P(d) = \frac{1}{d}\sum_{x=0}^{d} h(x) \tag{7.4}$$

In this instance, d may be thought of as the scale or step size, as a lower value will effectively result in a lower 'resolution' measure of the object perimeter and vice-versa. A plot of $\log P(d)$ versus $\log d$ produces a straight line (Fig. 7.3). However, such an approach is not suitable for the analysis of hyphae, as the EDM of such images typically contains a very small number of grey levels due to the elongated nature of hyphae.

The 'box-counting' method has been by far the most common in the analysis of filamentous microbes [24]. This approach entails covering the mycelium with a grid of side length ϵ and counting the number of boxes, $N(\epsilon)$, that are intersected by the mycelium. If the mycelium is a true fractal, then a relationship of the following form should be found:

$$N(\epsilon) = c\epsilon^{-D} \tag{7.5}$$

where c is a proportionality constant. The fractal nature of mycelia has been studied at two distinct levels using the measures of the surface fractal dimension (D_{BS}), effectively allowing discrimination between systems which are fractal only at their boundaries, and the mass fractal dimension (D_{BM}) [10, 24]. However, it has been suggested that the fractal dimension is often not sufficient for morphological characterisation, as microorganisms can

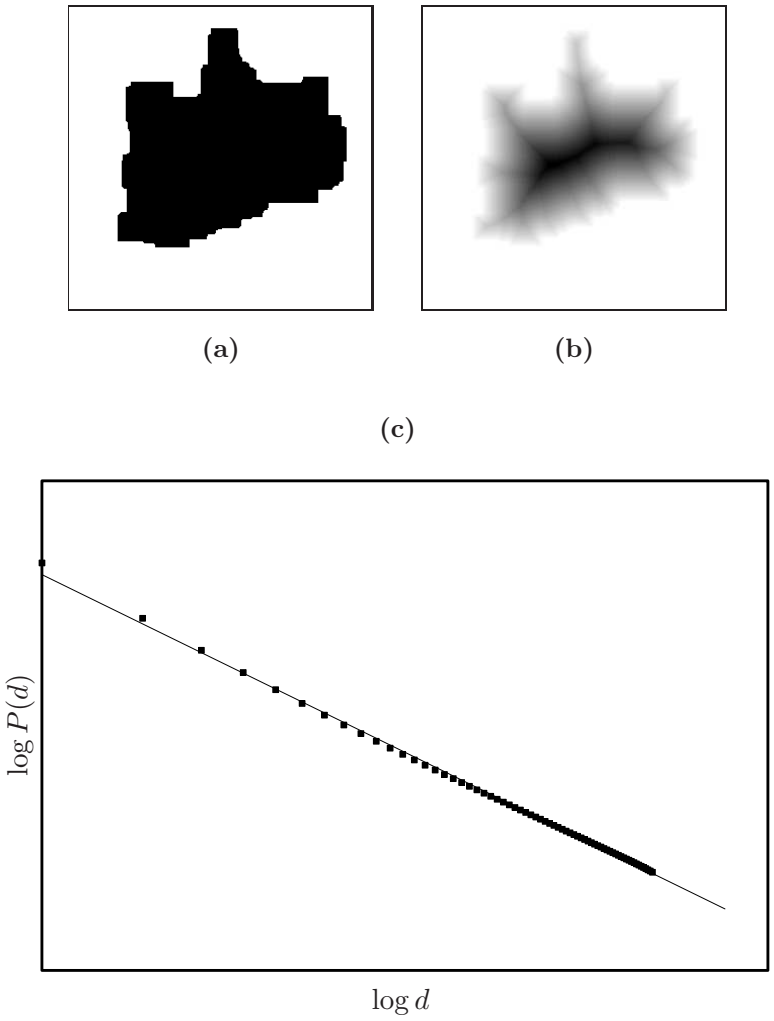

Figure 7.3: Enumeration of the fractal dimension based on the Euclidean distance map.

sometimes appear to have different branching patterns, despite having similar values for fractal dimension [25].

7.1.3 Aim: To relate fractal dimension to the hyphal growth unit by treating the mycelial boundary as a fractal curve

While numerous studies have been conducted in which fractal analysis is utilised to quantify morphology, few have attempted to link fractal dimension with conventional morphological parameters. Fractal analysis is of significant potential value in the study of

filamentous microorganisms, particularly as it lends itself to the quantification of all gross morphological forms that may be encountered. However, there is a need to develop further the relationship between the fractal dimension within a population of mycelia and the branching behaviour within that population. Here an alternative approach to fractal analysis is described, which directly relates the hyphal growth unit to the fractal dimension, based on an analysis of the mycelial boundary.

7.2 Materials & Methods

7.2.1 Inoculum preparation

Penicillium chrysogenum (IMI 321325) spores were harvested from malt agar (Lab M) slant cultures by addition of 5 ml phosphate-buffered saline (PBS; pH 7.2, Oxoid Dulbecco 'A'; 0.85% w/v) containing Tween 80 (0.1% v/v). Conidiospores were dislodged using a sterile swab, briefly mixed, and the suspension was filtered through sterile glass wool to remove hyphae. The inoculum was standardized using a Neubauer chamber to yield a stock concentration of 2×10^6 spores ml^{-1}, glycerol added to a final concentration of 20% (v/v) and aliquots stored at -20°C. The viability of spores after freezing was found to be approximately 47% of stock concentration (pour plate method, malt agar, 36 h incubation).

7.2.2 Microorganism cultivation

The basal medium used for solid state fermentation of *A. oryzae* was as described in Section 2.3 with 10.0 g L^{-1} Soluble Starch and 17.0 g L^{-1} Agar No. 1. Nonidet P-40 or Triton X-100 were added to yield a final concentration of either 0.1% or 5.0% w/v. The media was adjusted to pH 6.0 before autoclaving. Solid state fermentation of *P. chrysogenum* was carried out using the following: malt agar, malt agar supplemented

with $CaCl_2.2H_2O$ (0.08% w/v) or $FeCl_2.4H_2O$ (0.11% w/v), rice, orange and a mixture of rice and bulgar wheat (1:1 w/w). Rice and rice-bulgar wheat were prepared by steeping in water and autoclaving (121°C for 15 minutes) before transfer to sterile Petri dishes. Orange was prepared for use by surface swabbing with alcohol and dissection with a sterile knife. Cell immobilisation, cultivation conditions and processing of culture for image analysis were as described in Section 2.4.

Submerged fermentation of *A. oryzae* was carried out in a 2 L Benchtop Fermentor (BioFlo 110, New Brunswick Scientific). The approximate internal diameter of the vessel was 0.13 m and it had a working volume of 1.5 L. Agitation was provided by two Rushton turbines with a D/T ratio of 0.4 operated at 200 rpm. A pipe sparger was used to aerate the culture at an initial rate of 1.0 vvm. The fermentor was run without dissolved oxygen or pH control and the broth temperature was maintained at 30°C. Inoculum work-up consisted of three shake flask cultures (250 ml, 20% working volume) inoculated with 5×10^7 spores ml^{-1} and incubated at 30°C (200 rpm for 48 hours). The medium used for fermentation and inoculum work-up was as described above (Agar No. 1 and detergents omitted). Sample preparation for fluorescent microscopy and image capture were as described in Section 2.4.

7.2.3 Enumerating the fractal dimension

In all cases, only 'free' mycelial elements, exhibiting minimal overlapping of hyphae, were considered for image analysis, so that comparisons could be drawn between the fractal dimension and the hyphal growth unit. The generation of binary images and the enumeration of the hyphal growth unit were as described in Chapter 3. In the case of calcofluor white-stained samples, a pre-set grey-level threshold was used, as the non-uniform nature of the stain uptake complicated automated segmentation.

The fractal dimension, D, of an object, O, was determined by first locating the object boundary in a binary image (all foreground pixels bordering background), which can be

thought of as a fractal curve, consisting of a set of N coordinates, (x_n, y_n). From this series of points, a 'fractal signal' [26], $f(n)$, can be constructed as follows:

$$f(n) = \sqrt{(x_n - x_c)^2 + (y_n - y_c)^2} \quad \text{for all} \quad 0 < n < N \tag{7.6}$$

where (x_c, y_c) is the average location of all $(x, y) \in O$ (Fig. 7.4). If $f(n)$ is a fractal signal, then the following relationship holds true:

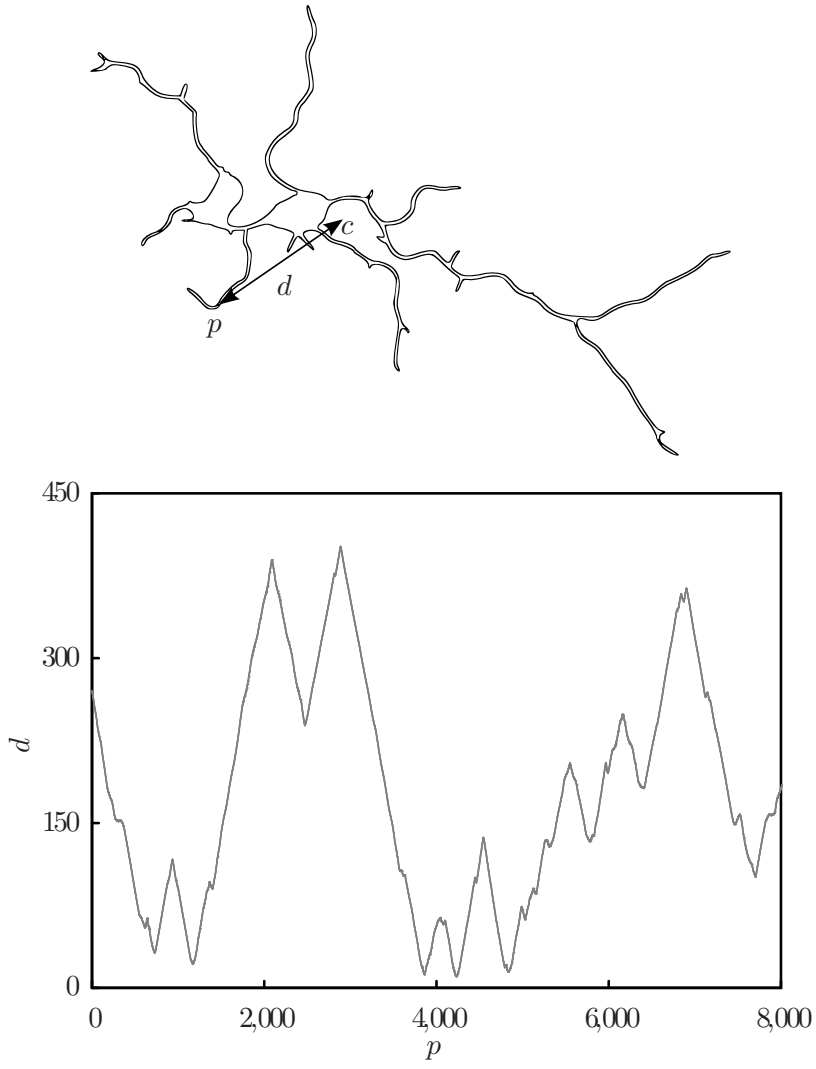

Figure 7.4: Illustration of algorithm for determination of fractal dimension of mycelial structures. Distance, d, between the centroid, c, and the boundary is plotted for each position on the boundary, p.

$$P(\omega) = \frac{c}{\omega^{\beta}} \tag{7.7}$$

where $P(\omega) = |F(\omega)|^2$, $F(\omega)$ is the Fourier transform of $f(n)$, $\beta = 2q$, q is the Fourier Dimension and c is a constant. Taking the log of this equation yields:

$$\log P(\omega) = -\beta \log \omega + c \tag{7.8}$$

D is related to β by [26]:

$$D = \frac{5 - \beta}{2} \tag{7.9}$$

A value for β can therefore be determined by linear regression of a plot of $\log P(\omega)$ against $\log \omega$, excluding the DC component (Fig. 7.5). All algorithms were implemented in Java using ImageJ [27].

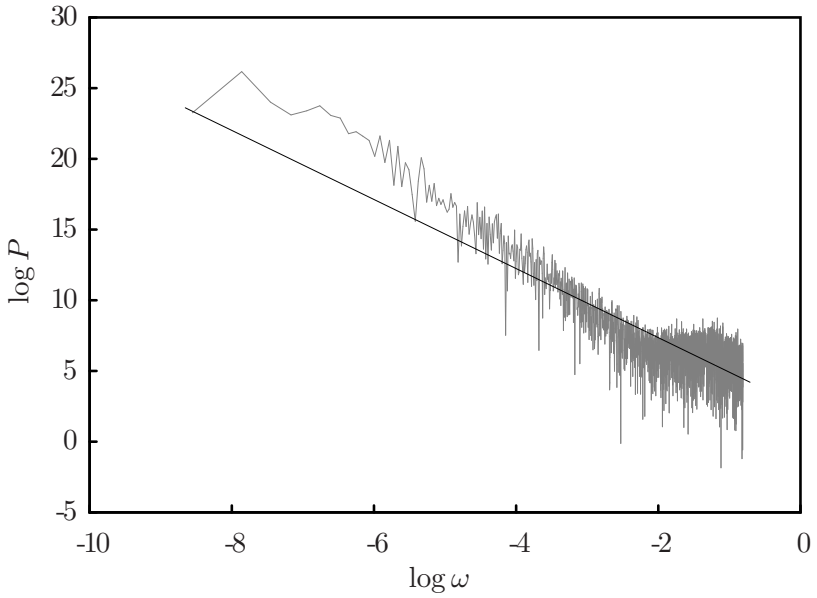

Figure 7.5: Illustration of algorithm for determination of fractal dimension of mycelial structures. The fractal dimension is derived from a log-log plot of the Fourier domain representation of the signal.

7.3 Results & Discussion

An analysis of the development of *A. oryzae* on malt agar showed that both D and L_{hgu} increased over time and both tended towards approximately constant values (Fig. 7.6). This suggests that the value of L_{hgu} specific to *A. oryzae* under these growth conditions is reflected in the fractal dimension of the mycelia. The fractal dimension of *Ashbya gossypii* and *Streptomyces griseus* were also found to increase with time during the colonisation of solid substrates [24]. *A. oryzae* and *P. chrysogenum* were grown under a variety of different conditions (Table 7.1), producing mycelia of varying size and dimension that were quantified in the same manner. The resultant mean values of D obtained for each population were plotted against the mean values of L_{hgu} to yield an approximately logarithmic relationship (Fig. 7.7):

$$D = a \log L_{hgu} + b \tag{7.10}$$

where a and b are constants. This result demonstrates a strong correlation between the branching behaviour of mycelia and their space-filling properties. However, it has been shown in other studies that fractal dimension tends to increase as projected area of mycelial structures increases [10]. This may also be the case in this study, as higher values of D tended to be biased toward high values of A_p (Fig. 7.8), but this result is inconclusive, as the sizes of mycelia analysed fell within a relatively small range.

This result demonstrates a clear relationship between the branching behaviour of filamentous organisms and the fractal dimension of the resultant mycelial structures, further emphasising the potential use of fractal analysis in morphological quantification. An ability to extract information on the branching behaviour of an organism by analysing the shape of the mycelial boundary would be highly advantageous in the study of more complex conformations where measures such as the hyphal growth unit are not readily obtainable. Furthermore, as has been demonstrated in other studies [10, 11, 13, 20], frac-

Table 7.1: Populations of filamentous fungi analysed, where n is the number of mycelia in each population and the total hyphal length (L_{th}) is presented as mean ± 95% confidence interval

Organism	t (h)	Substrate	n	L_{th} (μm)
A. oryzae	14.0	Malt Agar[1]	86	85 ± 16
A. oryzae	15.4	Malt Agar	87	117 ± 21
A. oryzae	16.9	Malt Agar	82	169 ± 41
A. oryzae	18.3	Malt Agar	78	341 ± 71
A. oryzae	19.7	Malt Agar	83	305 ± 66
A. oryzae	21.1	Malt Agar	67	428 ± 98
A. oryzae	22.6	Malt Agar	59	336 ± 101
A. oryzae	24.0	Malt Agar	76	397 ± 91
A. oryzae	18.0	Solid medium, Nonidet P-40 5.0% (w/v)	30	190 ± 44
A. oryzae	24.0	Solid medium, Nonidet P-40 5.0% (w/v)	26	654 ± 177
A. oryzae	15.0	Solid medium, Triton X-100 0.1% (w/v)	44	177 ± 39
A. oryzae	18.0	Solid medium, Triton X-100 0.1% (w/v)	35	269 ± 95
A. oryzae	46.0	Submerged Medium	38	874 ± 198
A. oryzae	72.5	Submerged Medium	56	671 ± 116
A. oryzae	94.0	Submerged Medium	44	527 ± 126
P. chrysogenum	20.0	Malt Agar	69	116 ± 18
P. chrysogenum	27.0	Malt Agar	46	378 ± 73
P. chrysogenum	20.0	Malt Agar, $CaCl_2.2H_2O$ 0.08% (w/v)	68	131 ± 20
P. chrysogenum	27.0	Malt Agar, $CaCl_2.2H_2O$ 0.08% (w/v)	32	296 ± 52
P. chrysogenum	27.0	Malt Agar, $FeCl_2.4H_2O$ 0.11% (w/v)	58	140 ± 26
P. chrysogenum	20.0	Orange	39	180 ± 36
P. chrysogenum	19.0	Rice	114	255 ± 31
P. chrysogenum	20.0	Rice & Bulgar Wheat	42	400 ± 121

[1] Results for *A. oryzae* on malt agar were produced using the images generated in Chapter 5.

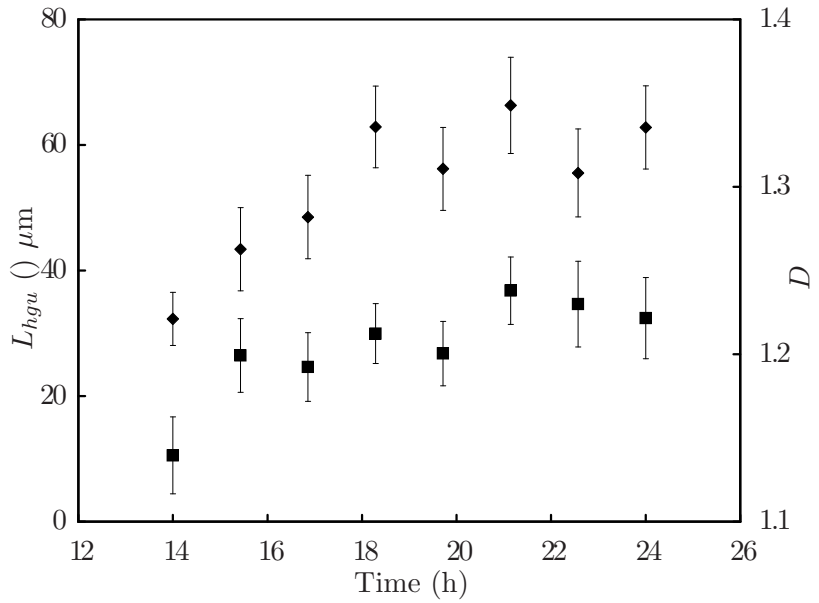

Figure 7.6: Temporal variation in mean hyphal growth unit (L_{hgu}; ♦) and the mean fractal dimension (D; ■) of populations of *A. oryzae* cultivated on malt agar. Error bars represent 95% confidence intervals.

tal analysis can be applied regardless of the gross morphological form that results in a particular process, allowing a more thorough compilation of data. However, a more complete analysis, including more complex structures, is necessary to validate the universal application of fractal analysis.

It has been previously suggested that the box-counting method of fractal dimension enumeration may not be suitable for the analysis of small, relatively unbranched hyphal structures [10, 24]. The accuracy of the box-counting method relies on an object being sufficiently great in size so as to allow a reasonably large variation in ϵ (approximately one order of magnitude has been suggested [24]). Given a value of approximately 4μm for ϵ_{min} (hyphal width is approximately 2-4μm), this suggests a minimum value of approximately 40μm for ϵ_{max} in this study, equating to a minimum object 'diameter' of 160μm. However, mycelia smaller than this dimension were often encountered, particularly in the case of *P. chrysogenum*. Further, the number of evaluations of $N(\epsilon)$ is restricted by the image

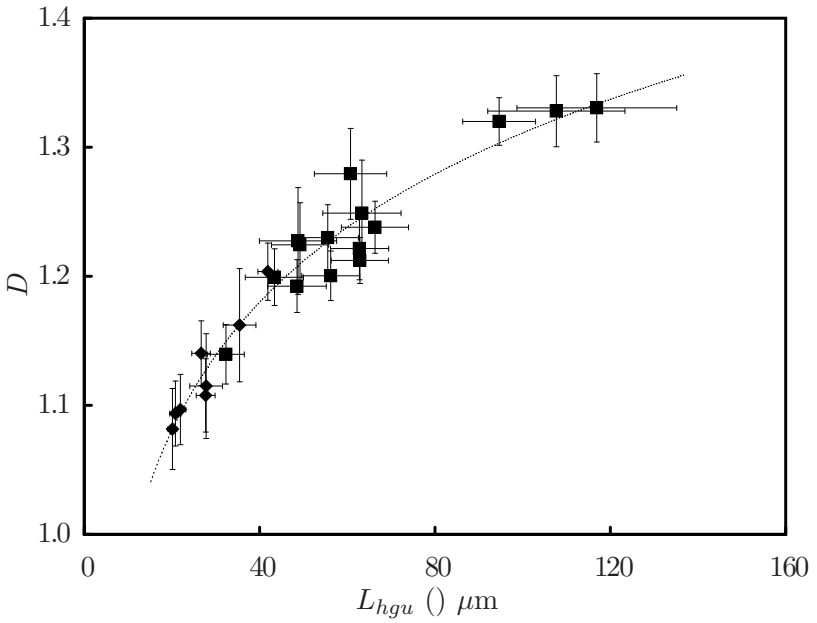

Figure 7.7: Relationship between the mean hyphal growth unit (L_{hgu}) and the mean fractal dimension (D) of populations of *Aspergillus oryzae* (■) and *Penicillium chrysogenum* (♦) mycelia, grown under a variety of different conditions. A logarithmic relationship of the form $D = a \log L_{hgu} + b$ exists between the two parameters, where $a = 0.14$ and $b = 0.65$ (—; $R^2 = 0.95$). Error bars represent 95% confidence intervals.

resolution (approximately 1μm per pixel in this study). This can obviously be overcome by increasing the image resolution, but this in turn results in a significant increase in memory usage and processing time.

By enumerating the fractal dimension based on the object boundary, considerations of resolution are obviated to some degree, as the boundary can be represented geometrically as a series of equations, or indeed as a single spline, to be sampled as often as is necessary to provide sufficient signal resolution. However, image resolution is still an important consideration, as low-resolution images may not contain an accurate representation of the object boundary. Consideration must also be given to the means used to locate the boundary. In this study, hyphae were uniformly stained and object segmentation from background was accurately performed by grey-scale thresholding. In cases where

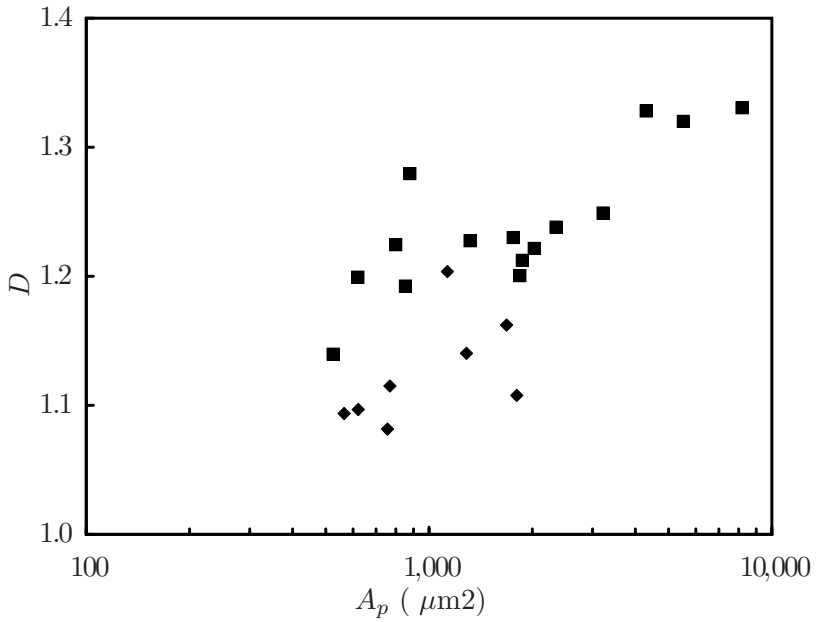

Figure 7.8: Relationship between mean fractal dimension (D) of populations of *Aspergillus oryzae* (■) and *Penicillium chrysogenum* (♦) mycelia and mean projected area (A_p).

staining is non-uniform, thresholding may not be suitable and some form of edge-detection algorithm may be required.

A similar examination of spectral periodicity was employed by Jones and colleagues in their study of the positional correlation between acid phosphatase intracellular concentration and hyphal cellular differentiation in *Pycnoporus cinnabarinus*. Acid phosphatase was detected histochemically on membrane-bound colonies, which were imaged using a camera fitted with a macro-lens. In the resulting image, a series of one-dimensional 'walks' were made along random colony radii and the fractal dimension calculated according to the power spectrum of the resultant luminance profile along each 'walk'. Different concentrations of an organic dye were used to effect substrate induction of the enzyme response, which was shown to be statistically correlated according to a fractal power law [28].

While numerous studies have been conducted in which fractal analysis is utilised to quantify mycelial morphology, few have attempted to link fractal dimension with conven-

tional morphological parameters. However, links have been established between fractal dimension and productivity in some processes. For example, in the optimisation of *Funalia trogii* fermentations, both fractal dimension and mean pellet area were monitored; while no link was established between the two parameters, it was suggested that a correlation may exist between fractal dimension and decolourisation of reactive black 5 [11]. A positive correlation was also found between fractal dimension and phenol-oxidase expression by *Pycnoporus cinnabarinus*, with both parameters being regulated by media composition [12].

Where links between fractal dimension and conventional Euclidean measures of morphology have been made, the relationship is often either ambiguous or qualitative in nature. An approximate correlation ($R^2 = 0.614$) was found between the convexity (defined as the ratio between convex perimeter and respective perimeter) of *Cupriavidus necator* DSM 545 flocs and D_{BS} [29]. Fractal dimension was shown to be related to broth rheology in the submerged fermentation of *Cephalosporium acremonium* M25 and a relationship with other morphological measures, such as the number of arthrospores in the media, was also suggested, but not explicitly demonstrated [13]. A relationship between hyphal growth unit and fractal dimension of mycelia was previously noted in submerged fermentations of *Aspergillus niger*, but the differences in the recorded values of L_{hgu} were ambiguous [14]. Further studies of *A. niger* revealed that medium composition had a significant impact on the fractal dimension, the changes in morphology reflected in variations in the size and compactness of mycelial aggregates [10]. The local fractal dimension (determined by the concentric circles method) within a colony of *Trichoderma viride* was found to increase with branching frequency (occurrence of 'loops' in the mycelium), although the result was rather qualitative in nature [15]. However, successful attempts have been made in relating fractal dimension to growth kinetics. While colony expansion rates were found to differ between different strains of *Cryphonectria parasitica*, fractal dimension was found to correlate with the expansion rate, independent of strain [16].

7.4 Conclusion

The optimisation of industrial fermentation processes involving filamentous microbes requires extensive knowledge of morphological development, as productivity is heavily influenced by the specific phenotypic form adopted by an organism in a certain process. The accurate quantification of morphological variation in vegetative mycelia is therefore of the utmost importance, but the characterisation of complex morphologies represents a significant challenge. The utility of conventional measures employed in the analysis of these microbes (such as projected area, perimeter length and circularity) is limited, as they reveal little about the extent of branching of the organism, which is known to be related to metabolite production.

An alternative approach to morphological quantification employs the use of fractal geometry to characterise the spatial distribution of an organism. The self-similar nature of mycelial structures has been demonstrated in numerous studies and there is clearly significant potential benefit in the application of fractal analysis to filamentous microorganisms. What has been lacking in these studies is a firm link between fractal dimension and conventional morphological parameters, such as the hyphal growth unit. This study indicates a strong correlation between these two parameters in the analysis of 'free' mycelial elements and further investigation involving a wide range of complex conformations is necessary. Future work will focus on elucidating a universal relationship between fractal dimension, branching behaviour and productivity, independent of the gross morphological form encountered in a given process. It is hoped that this work will lead to a rapid and efficient means of morphological quantification for use in industrial processes.

References

[1] P. Žnidaršič and A. Pavko, "The morphology of filamentous fungi in submerged cultivations as a bioprocess parameter," *Food technol. biotechnol.*, vol. 39, no. 3, pp. 237–252, 2001.

[2] C. L. Gordon, D. B. Archer, D. J. Jeenes, J. H. Doonan, B. Wells, A. P. Trinci, and G. D. Robson, "A glucoamylase::GFP gene fusion to study protein secretion by individual hyphae of *Aspergillus niger*," *J Microbiol Methods*, vol. 42, no. 1, pp. 39–48, 2000, doi: 10.1016/S0167-7012(00)00170-6.

[3] C. Müller, M. McIntyre, K. Hansen, and J. Nielsen, "Metabolic engineering of the morphology of *Aspergillus oryzae* by altering chitin synthesis," *Appl Environ Microbiol*, vol. 68, no. 4, pp. 1827–36, 2002, doi: 10.1128/AEM.68.4.1827-1836.2002.

[4] M. Papagianni and M. Mattey, "Physiological aspects of free and immobilized *Aspergillus niger* cultures producing citric acid under various glucose concentrations," *Process Biochemistry*, vol. 39, no. 12, pp. 1963–1970, 2004, doi: 10.1016/j.procbio.2003.09.027.

[5] M. Carlsen, A. B. Spohr, J. Nielsen, and J. Villadsen, "Morphology and physiology of an alpha-amylase producing strain of *Aspergillus oryzae* during batch cultivations," *Biotechnol Bioeng*, vol. 49, no. 3, pp. 266–76, 1996, doi: 10.1002/(SICI)1097-0290(19960205)49:3<266::AID-BIT4>3.0.CO;2-I.

[6] M. Papagianni and M. Mattey, "Morphological development of *Aspergillus niger* in submerged citric acid fermentation as a function of the spore inoculum level. Application of neural network and cluster analysis for characterization of mycelial morphology," *Microb Cell Fact*, vol. 5, no. 1, p. 3, 2006, doi: 10.1186/1475-2859-5-3.

[7] K. G. Tucker, T. Kelly, P. Delgrazia, and C. R. Thomas, "Fully-automatic measurement of mycelial morphology by image analysis," *Biotechnol. Prog.*, vol. 8, no. 4, pp. 353–359, 1992, doi: 10.1021/bp00016a013.

[8] Z. J. Li, V. Shukla, K. S. Wenger, A. P. Fordyce, A. G. Pedersen, and M. R. Marten, "Effects of increased impeller power in a production-scale *Aspergillus oryzae* fermentation," *Biotechnol Prog*, vol. 18, no. 3, pp. 437–44, 2002, doi: 10.1021/bp020023c.

[9] B. B. Mandelbrot, *The fractal geometry of nature*. New York: W.H. Freeman, 1982.

[10] M. Papagianni, "Quantification of the fractal nature of mycelial aggregation in *Aspergillus niger* submerged cultures," *Microb Cell Fact*, vol. 5, no. 1, p. 5, 2006, doi: 10.1186/1475-2859-5-5.

[11] C. Park, J.-S. Lim, Y. Lee, B. Lee, S.-W. Kim, J. Lee, and S. Kim, "Optimization and morphology for decolorization of reactive black 5 by *Funalia trogii*," *Enzyme and Microbial Technology*, vol. 40, no. 7, pp. 1758–1764, 2007, doi: 10.1016/j.enzmictec.2006.12.005.

[12] C. L. Jones and G. T. Lonergan, "Prediction of phenol-oxidase expression in a fungus using the Fractal Dimension," *Biotechnology Letters*, vol. 19, no. 1, pp. 65–69, 1997, doi: 10.1023/A:1018371121663.

[13] J. C. Kim, J. S. Lim, J. M. Kim, C. Kim, and S. W. Kim, "Relationship between morphology and viscosity of the main culture broth of *Cephalosporium acremonium* M25," *Korea-Australia Rheology Journal*, vol. 17, no. 1, pp. 15–20, 2005.

[14] D. Ryoo, "Fungal fractal morphology of pellet formation in *Aspergillus niger*," *Biotechnology Techniques*, vol. 13, no. 1, pp. 33–36, 1999, doi: 10.1023/A:1008835529941.

[15] D. Hitchcock, C. A. Glasbey, and K. Ritz, "Image analysis of space-filling by networks: Application to a fungal mycelium," *Biotechnology Techniques*, vol. 10, no. 3, pp. 205–210, 1996, doi: 10.1007/BF00158947.

[16] M. R. Golinski, W. J. Boecklen, and A. L. Dawe, "Two-dimensional fractal growth properties of the filamentous fungus *Cryphonectria parasitica*: the effects of hypovirus infection," *Journal of Basic Microbiology*, vol. 48, no. 5, pp. 426–429, 2008, doi: 10.1002/jobm.200800017.

[17] T. Matsuyama and M. Matsushita, "Self-similar colony morphogenesis by gram-negative rods as the experimental model of fractal growth by a cell population," *Appl. Environ. Microbiol.*, vol. 58, no. 4, pp. 1227–1232, 1992.

[18] C. Kampichler, J. Rolschewski, D. P. Donnelly, and L. Boddy, "Collembolan grazing affects the growth strategy of the cord-forming fungus *Hypholoma fasciculare*," *Soil Biology and Biochemistry*, vol. 36, no. 4, pp. 591–599, 2004, doi: 10.1016/j.soilbio.2003.12.004.

[19] J. M. Wells, M. J. Harris, and L. Boddy, "Encounter with new resources causes polarized growth of the cord-forming basidiomycete *Phanerochaete velutina* on soil," *Microbial Ecology*, vol. 36, no. 3, pp. 372–382, 1998, doi: 10.1007/s002489900123.

[20] C. L. Jones, G. T. Lonergan, and D. E. Mainwaring, "Mycelial fragment size distribution: an analysis based on fractal geometry," *Applied Microbiology and Biotechnology*, vol. 39, no. 2, pp. 242–249, 1993, doi: 10.1007/BF00228613.

[21] B. Mandelbrot, "How long is the coast of Britain? Statistical self-similarity

and fractional dimension," *Science*, vol. 156, no. 3775, pp. 636–38, May 1967, doi: 10.1126/science.156.3775.636.

[22] L. F. Richardson, "The problem of contiguity: An appendix to statistic of deadly quarrels," in *General systems: Yearbook of the Society for the Advancement of General Systems Theory*. Ann Arbor, Michigan: Society for General Systems Research, 1961, vol. 6, pp. 139–87.

[23] J. C. Russ, *The image processing handbook*, 4th ed. Boca Raton, Florida: CRC Press, 2002.

[24] M. Obert, P. Pfeifer, and M. Sernetz, "Microbial growth patterns described by fractal geometry," *J Bacteriol*, vol. 172, no. 3, pp. 1180–5, 1990.

[25] L. Boddy and D. P. Donnelly, "Fractal geometry and microorganisms in the environment," in *Biophysical chemistry of fractal structures and processes in environmental systems*. Chichester: John Wiley and Sons, 2008, pp. 239–272.

[26] J. M. Blackledge, *Digital Image Processing*, 1st ed. Chichester: Horwood Publishing, 2005.

[27] W. S. Rasband, "ImageJ," 1997-2009, URL: http://rsbweb.nih.gov/ij.

[28] C. L. Jones, G. T. Lonergan, and D. E. Mainwaring, "Acid phosphatase positional correlations in solid surface fungal cultivation: A fractal interpretation of biochemical differentiation," *Biochemical and Biophysical Research Communications*, vol. 208, no. 3, pp. 1159–65, 1995, doi: 10.1006/bbrc.1995.1455.

[29] L. Finkler, Y. Ginoris, C. Luna, T. Alves, J. Pinto, and M. Coelho, "Morphological characterization of *Cupriavidus necator* DSM 545 flocs through image analysis," *World Journal of Microbiology and Biotechnology*, vol. 23, no. 6, pp. 801–808, 2007, doi: 10.1007/s11274-006-9300-8.